Exchangeability of Alpha-Actinin in Living Cardiac Fibroblasts and Muscle Cells

NANCY M. McKENNA,* JAMES B. MEIGS,* and YU-LI WANG*‡
*Department of Molecular and Cellular Biology, National Jewish Hospital and Research Center, Denver, Colorado 80206, and ‡Department of Biochemistry, Biophysics and Genetics, University of Colorado Health Services Center, Denver, Colorado 80220.

ABSTRACT We have investigated the exchangeability of alpha-actinin in various structures of cultured chick cardiac fibroblasts and muscle cells using fluorescent analogue cytochemistry in combination with fluorescence recovery after photobleaching. Living cells were microinjected with tetramethylrhodamine-labeled alpha-actinin, which became localized in cellular structures. Small areas of labeled structures were then photobleached with a laser pulse, and the subsequent recovery of fluorescence was monitored with an image intensifier coupled to an image-processing system. In fibroblasts, fluorescence recovery was studied in stress fibers and in adhesion plaques. Bleached spots in adhesion plaques generally attained complete recovery within 20 min; whereas complete recovery in stress fibers occurred within 30 to 60 min. In muscle cells, alpha-actinin became localized in the Z-lines of sarcomeres, in punctate structures, and in apparently continuous bundle-like structures. Fluorescence recovery in Z-lines, punctate structures, and some bundle-like structures was extremely slow. Complete recovery did not occur within the 6- to 7-h observation period. However, some bundle-like structures recovered completely within 60 min, a rate similar to that of stress fibers in fibroblasts. These results indicate that fluorescently labeled alpha-actinin is more stably associated with structures in muscle cells than in fibroblasts. In addition, different structures within the same cell can display different alpha-actinin exchangeabilities which, in muscle cells, could be developmentally related.

The dynamic properties of cytoskeletal proteins such as actin, alpha-actinin, and tubulin in living cells have been studied recently in a number of laboratories (9, 15, 16, 20, 25, 28, 30). Even at steady state, a constant exchange seems to occur between molecules associated with cellular structures and those diffusible in the cytoplasm (9, 16, 20, 25, 30). It is not clear, however, how this dynamic equilibrium is maintained and what factor(s) affect the exchangeability of proteins in different structures and cell types.

A particularly interesting question is the relative exchangeability of proteins associated with stress fibers in fibroblasts, and those associated with myofibrils in muscle cells. Previous studies have pointed out a number of structural and functional similarities between stress fibers and myofibrils. For example, stress fibers contain many of the contractile proteins, including actin, myosin, alpha-actinin, and tropomyosin, which are present in myofibrils. In addition, the spatial relationships of these proteins are similar in both structures (11,

21). It has also been demonstrated that stress fibers can contract both in cell models (15) and in living cells (14, 28) under some conditions. However, stress fibers are also different from myofibrils in several important aspects including the mixed polarity of actin filaments (2), the absence of prominent myosin filaments (10), and the ability to undergo rapid reorganization (28).

In this study, we have used fluorescent analogue cytochemistry (26, 29) in combination with fluorescence recovery after photobleaching (FRAP)[1] to compare the exchangeability of alpha-actinin in various structures in embryonic fibroblasts and cardiac muscle cells. It has been demonstrated that the cellular localization of injected fluorescent analogues including actin, alpha-actinin, and tropomyosin correlates closely with that of the endogenous counterparts (for review see

---

[1] Abbreviations used in this paper: FRAP, fluorescence recovery after photobleaching; ISIT camera, Intensified Silicon Intensified Target camera.

references 26 and 29). Moreover, these fluorescent analogues can participate in the reorganization of existing structures as well as the *de novo* assembly of new structures (28). Thus, injected analogues can function as accurate tracers for the distribution and behavior of endogenous proteins. Fluorescent analogue cytochemistry in combination with the FRAP technique has been used previously to study the mobility of proteins in the ground cytoplasm and in discrete cytoplasmic structures (9, 16, 20, 25, 30). At appropriate intensities, the laser beam only bleaches the fluorophore without disrupting the integrity of the structure (13, 25). The subsequent recovery of fluorescence thus reflects the exchange of intact protein molecules in and out of the bleached area.

To analyze both the rate and the spatial pattern of fluorescence recovery, we have used image intensification and digital image–processing techniques, which not only yield fluorescence images of high quality at very low levels of excitation, but also provide detailed quantitative data on the distribution of fluorescence intensities. We have observed that alpha-actinin is much more stably associated with muscle structures, such as the Z-lines of myofibrils, than it is with fibroblast stress fibers. In addition, our results indicate that different structures within both muscle cells and fibroblasts can exhibit different exchangeabilities of alpha-actinin.

MATERIALS AND METHODS

Preparation of Fluorescent Analogues: Smooth muscle alpha-actinin was isolated from frozen chicken gizzards (Pel-Freez Biologicals, Rogers, AR) according to the protocol of Feramisco and Burridge (7), with the following modification: after elution from a DE-52 column, the fractions containing alpha-actinin were pooled and fractionated with a hydroxyapatite column (DNA-grade, Bio-Gel HTP, Bio-Rad Laboratories, Richmond, CA), before further fractionation with a Sepharose 6B-CL column (Sigma Chemical Co., St. Louis, MO). Nonmuscle alpha-actinin was isolated from frozen calf thymus by essentially the same protocol with the following minor modification: after the first extraction and up to the first ammonium sulfate cut, the solution was titrated to pH 7.0 before each clarification to reduce the viscosity of the solution. Purified thymus and smooth muscle alpha-actinins exhibited identical behavior on the Sepharose 6B-CL column and on SDS gels. Both alpha-actinins were concentrated by vacuum dialysis against 1 mM PIPES, 0.02% NaN₃, pH 7.0, and stored in liquid nitrogen at 13–15 mg/ml.

During fluorescent labeling, iodoacetamidotetramethylrhodamine (Research Organics Inc., Cleveland, OH) was dissolved in 200 mM potassium borate buffer, pH 9.0, and clarified in a Beckman type 42.2 Ti rotor (Beckman Instruments, Inc., Palo Alto, CA) at 100,000 g for 20 min to remove undissolved dye aggregates. Stored alpha-actinin was thawed and mixed 1:1 (vol/vol) with the clarified dye solution. The molar ratio between the dye prior to clarification

and the protein was 20. After mixing, the solution was incubated at 0°C for 4 h, clarified, and applied to a 0.7 × 15-cm column of Bio-Beads SM-2 (Bio-Rad Laboratories) equilibrated with 2 mM Tris-Cl, pH 8.5, to remove unbound dye molecules. Fluorescent fractions in the void volume were pooled and concentrated by vacuum dialysis against injection buffer containing 1 mM PIPES, pH 6.95, to a concentration of 5 mg/ml. The conjugate had a final dye-to-protein subunit (100,000 dalton) molar ratio of 1.1 to 2.1, estimated using a molar extinction coefficient of 23,000 at 555 nm for bound tetramethylrhodamine. The range of labeling ratios did not affect our results.

The conjugate was stored up to 1 mo on ice and was clarified at 100,000 g for 20 min before microinjection. The purity of alpha-actinin and the absence of unbound dye were determined by SDS gel electrophoresis. The ability of alpha-actinin to cross-link actin filaments was determined by falling-ball viscometry (18). Labeled alpha-actinin from either source retained 100% of the cross-linking activity of the unlabeled protein. In addition, the cross-linking activity of both labeled and unlabeled thymus alpha-actinins was sensitive to the free calcium ion concentration: increase in viscosity was detected in the presence of 0.5 mM EGTA but not in the presence of 0.05 mM Ca²⁺.

Cell Culture, Microinjection, and Fluorescence Microscopy: Monolayer cultures of cardiac fibroblasts and muscle cells were obtained by trypsinizing hearts of 7-d-old chick embryos (5). Cells were plated on glass coverslips (28) and maintained in F12K medium (KC Biological, Inc., Lenexa, KS) with 5% fetal bovine serum (KC Biological, Inc.) and antibiotics. 1–5 d after plating, cells were microinjected as described previously (27, 28). Many muscle cells continued to beat during and after microinjection. It has been estimated that, using an alpha-actinin solution of 5 mg/ml, the method of microinjection increases the number of cellular alpha-actinin molecules by ~10% (27). The results reported were not affected by variations in the volume of microinjection.

After microinjection, the culture dish was incubated for 1–8 h before photobleaching to allow incorporation of injected molecules. The rate of recovery after photobleaching was not affected by the period of incubation. During photobleaching and observation, culture dishes were placed on the heated stage of a Zeiss IM-35 inverted microscope in a humidified atmosphere containing an appropriate level of CO₂. Fluorescence images were observed using a 100x Neofluar oil immersion objective (NA 1.30) and epi-illumination. A 100-W quartz-halogen lamp operated at 5–7 V (17–34% full power) was used as the light source. Neither the lamp voltage nor the position of the microscope stage was changed throughout each experiment. Fixation and fluorescent phallotoxin staining were performed according to Amato et al. (1).

The apparatus for laser photobleaching was similar to that described by Jacobson et al. (12). A 2-W argon ion laser (Lexel Corp., Palo Alto, CA), in conjunction with an electronic shutter (Vincent Associates, Rochester, NY) was used to generate the laser pulse.

Image Processing: Fluorescent images were detected with an Intensified Silicon Intensified Target (ISIT) (Dage-MTI, Michigan City, IN) camera coupled to an image-processing computer (G. W. Hannaway & Associates, Boulder, CO), which included a PDP 11/73 microcomputer, a 330-megabyte hard disk, image processing boards (three frame buffers, arithmetic logic unit, and analog processor) and a graphics tablet. Software for image processing was developed by G. W. Hannaway & Associates and by us. Fluorescence images of cells before photobleaching and at specified time points after bleaching were averaged and stored without further processing on the hard disk in a format of
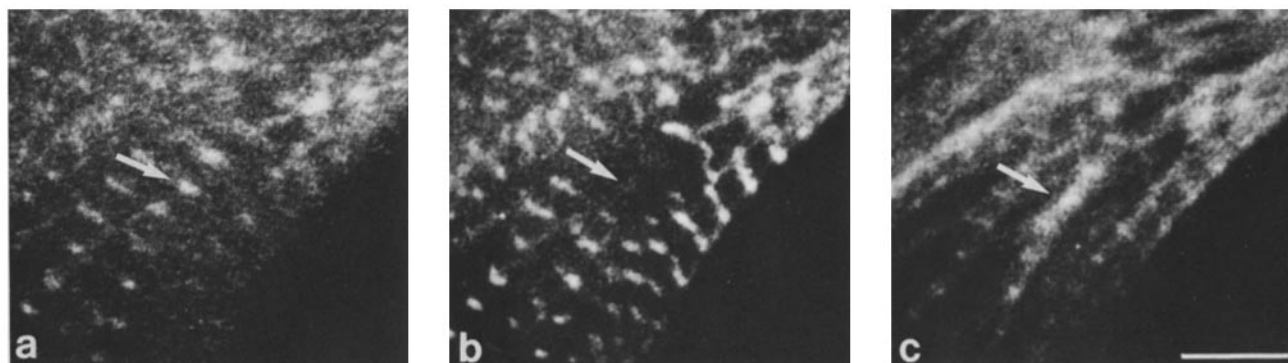

FIGURE 1   Comparison of tetramethylrhodamine alpha-actinin images of a microinjected cardiac muscle cell before and after photobleaching, with the fluorescein–phalloidin image of the same cell after photobleaching. The Z-lines (arrows) visible in the tetramethylrhodamine image before bleaching (a) are almost undetectable in the tetramethylrhodamine image after bleaching (b). The fluorescein–phalloidin image (c), however, shows a continuous, intact myofibril extending through the bleached spot. The cell in b and c has been fixed and extracted. Bar, 5 μm.

512 pixel × 480 pixel × 8 bit. The signal-to-noise ratio of the image was improved dramatically by averaging 64–128 frames. This allowed us to use extremely low levels of illumination and minimize photobleaching and light-induced cell damage during observation.

For visualization and photography of structures and bleached spots, background was subtracted from the image and the range of fluorescence intensities was expanded linearly. This procedure remarkably enhanced the contrast of the image. All images in a series were processed identically.

For quantitative measurements, fluorescence intensities in most experiments were determined by specifying an area in an averaged image using a graphics tablet (GTCO Corp., Rockville, MD) and calculating the average intensity within the delimited area. When the area of interest was too small to delimit with the tablet, the intensity of a single designated pixel or the average intensity in a 5-pixel × 5-pixel area surrounding a designated pixel was determined. The results were not affected appreciably by the method of data acquisition. For each experiment and for every time point, intensities were obtained at bleached
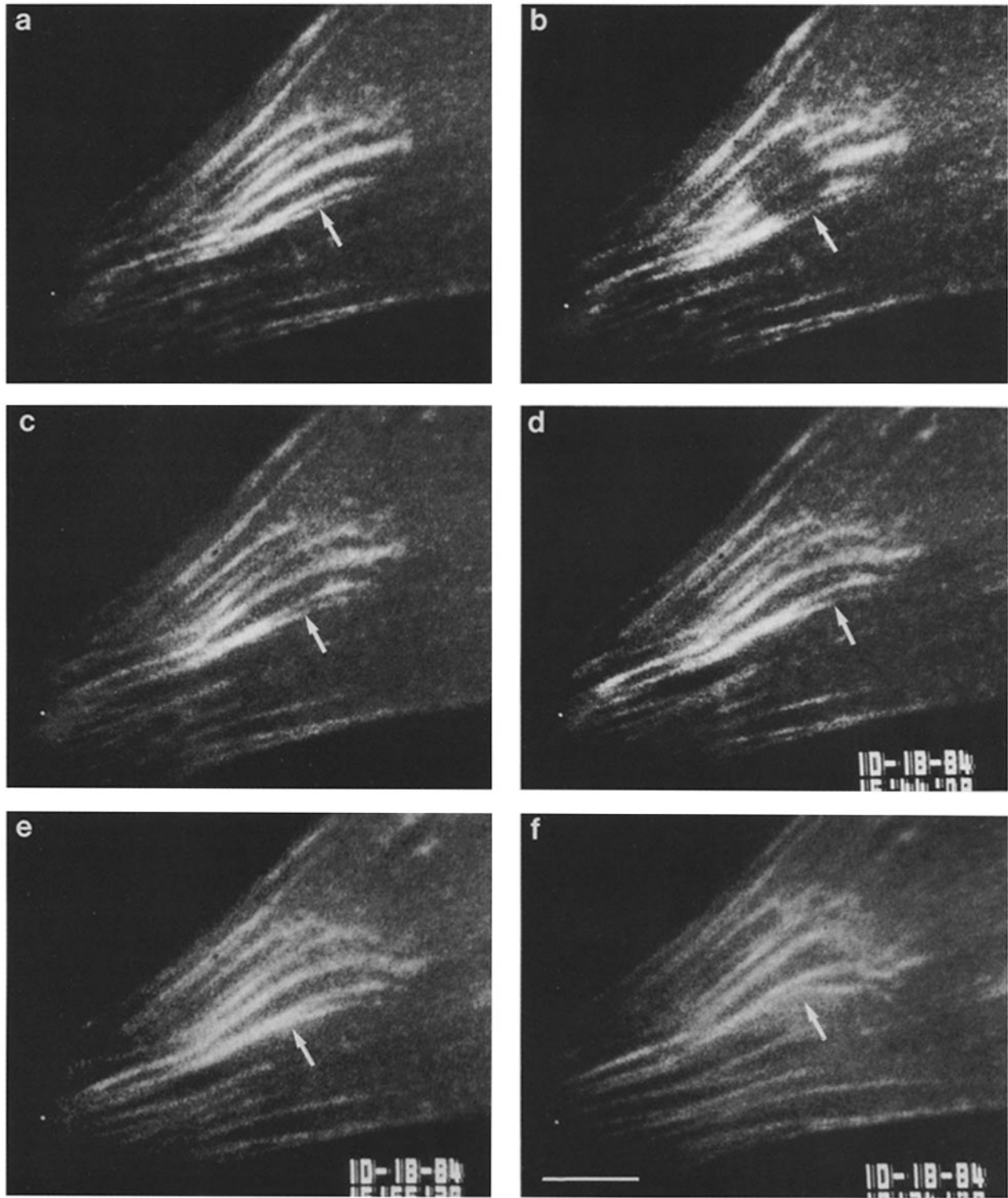
FIGURE 2 FRAP of stress fibers in a fibroblast. Arrows indicate the location of the bleached spot. Essentially complete recovery is reached at 60 min after bleaching (f). Fluorescence intensity before bleaching is designated 100% (a). Immediately after bleaching (b), fluorescence intensity equals 36%; 10 min after (c), 59%; 20 min (d), 60%; 30 min (e), 74%; 60 min (f), 103%. Bar, 10 μm.

spots, at constant unbleached structures, and in areas of diffuse fluorescence. The areas of measurement were selected as close to one another as possible. Intensities of bleached and unbleached structures were first adjusted by subtracting out the value measured in an area of diffuse fluorescence, in order to correct, to a first approximation, for the contribution from camera dark current, ground cytoplasm, and defocused light. Then fluorescence intensities of unbleached structures were used to normalize the intensities in bleached areas to correct for possible effects of slight changes in focusing and of photobleaching during observation. The ISIT camera was operated with the gamma correction circuitry disabled. By varying the excitation light from 12 to 100% with neutral density filters, we determined that the image intensifier has a linearity better than 95% over the range of operation. In addition, except for variations in fixed background values, essentially identical responses were obtained across the field.

RESULTS

Microinjected alpha-actinin became localized in cellular structures a short time after microinjection. Within 1–3 h, diffuse fluorescence decreased to a low level and incorporation reached an apparent steady state. In fibroblasts, injected alpha-actinin was localized in stress fibers, in adhesion plaques, and in membrane ruffles. In cardiac muscle cells, injected alpha-actinin was observed in the Z-lines of sarcomeres, in punctate structures, and also in apparently continuous bundle-like structures. The punctate structures were often arranged in a linear pattern and were continuous with myofibrils. Staining with fluorescent phalloidin indicated that both punctate regions and bundle-like structures also contained bundles of actin filaments (not shown).

Structures were photobleached with a 50-ms laser pulse at a power of 75 mW. The diameter of the bleached spot was between 1.5 and 5 μm. The degree of photobleaching was affected to some extent by the depth of the cell and the structure, but the rate of recovery was unaffected by the extent of photobleaching. Moreover, in no case was the laser pulse intense enough to sever or destroy the structure. Staining of photobleached cells with fluorescein–phalloidin, which specifically binds F-actin, indicated that the continuity of structures was maintained across bleached spots (Fig. 1). Frequently, photobleached myofibrils continued to contract throughout the experiments.

FRAP in Fibroblasts

Stress fibers were usually photobleached near the midpoint, or in the case of fibers which extended from one end of the cell to the other, at a point approximately equidistant between one end of the fiber and the nucleus. The recovery of fluorescence was analyzed both qualitatively by recording the images of the cell, and quantitatively by measuring the average fluorescence intensity of the bleached segment.

The outline of the bleached spot was well defined immediately after bleaching, but became less clear within 10 min (Fig. 2). However, the length of the bleached segment on a stress fiber did not change detectably during recovery, and fluorescence recovery appeared to occur simultaneously at all points along the bleached segment. The bleached spot often became undiscernable to the eye within 30 min (Fig. 2). However, quantitative analyses indicated that complete recovery was attained between 30 to 60 min after bleaching. Fig. 3 shows the time course of the recovery process. The recovery during the early period of observation occurred at a faster rate than that observed at later times. The half recovery time ($t_{1/2}$) was ~7 min. Recovery times for adjacent stress fibers in the same cell were very similar.
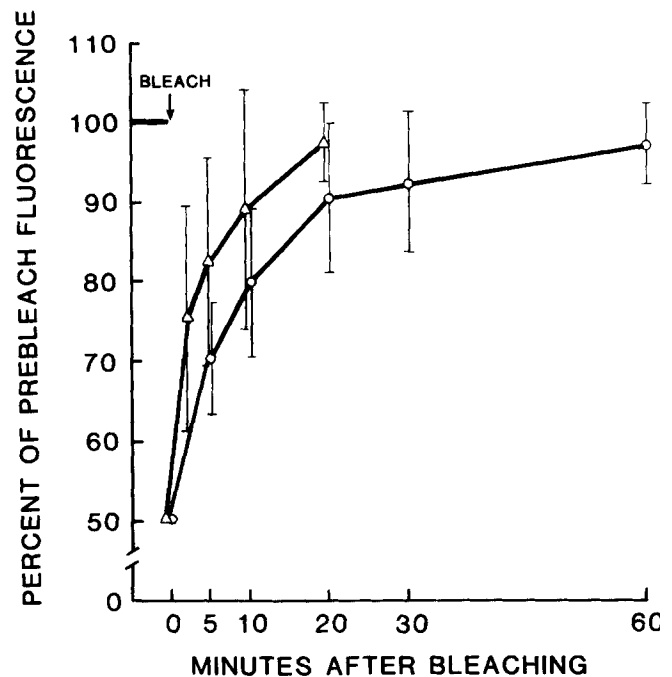

FIGURE 3 FRAP of fibroblast structures as a function of time. Fluorescence in adhesion plaques ($\triangle$) generally recovers within 20 min. Fluorescence in stress fibers (O) recovers within ~60 min. Data have been normalized to an initial bleach level of 50%. Values are the means ± SDs of 5–15 experiments.

We also studied the recovery at adhesion plaques, which were identified with interference reflection microscopy. These structures were or were not associated with stress fibers; they often underwent rapid changes in size or shape during the observation period. Fig. 4 shows the sequence of recovery after bleaching an adhesion plaque. Intensity measurements indicated that recovery in adhesion plaques was in general faster than that in stress fibers (Fig. 3). Fluorescence recovery was usually complete within 15 min, but in some cases took up to 30 min. The $t_{1/2}$ for adhesion plaques was ~3.5 min.

Since alpha-actinin in nonmuscle cells is thought to be regulated by the free calcium ion concentration (3), we were concerned that the use of gizzard alpha-actinin, which is not calcium sensitive, might induce artifacts in the measurement of mobility or exchangeability. Therefore, the same experiments were also performed with calcium-sensitive alpha-actinin purified from calf thymus. The results for both stress fibers and adhesion plaques were similar to those obtained using gizzard alpha-actinin (not shown).

FRAP in Cardiac Muscle Cells

Three classes of alpha-actinin–containing structures were photobleached in cardiac muscle cells: the Z-lines of sarcomeres, punctate structures, and apparently continuous bundle-like structures. When sarcomeres were photobleached, initial recovery was detectable within ~10 min. However, in no case was complete recovery ever detected within the 6- to 7-h observation period (Figs. 5 and 6). Results were similar whether a single Z-line or two to three Z-lines of a myofibril were bleached. As in fibroblast structures, recovery during the early period of observation occurred at a consistently faster rate than that observed at later times (Fig. 6). The $t_{1/2}$ for Z-lines was estimated to be between 6 and 13 h.
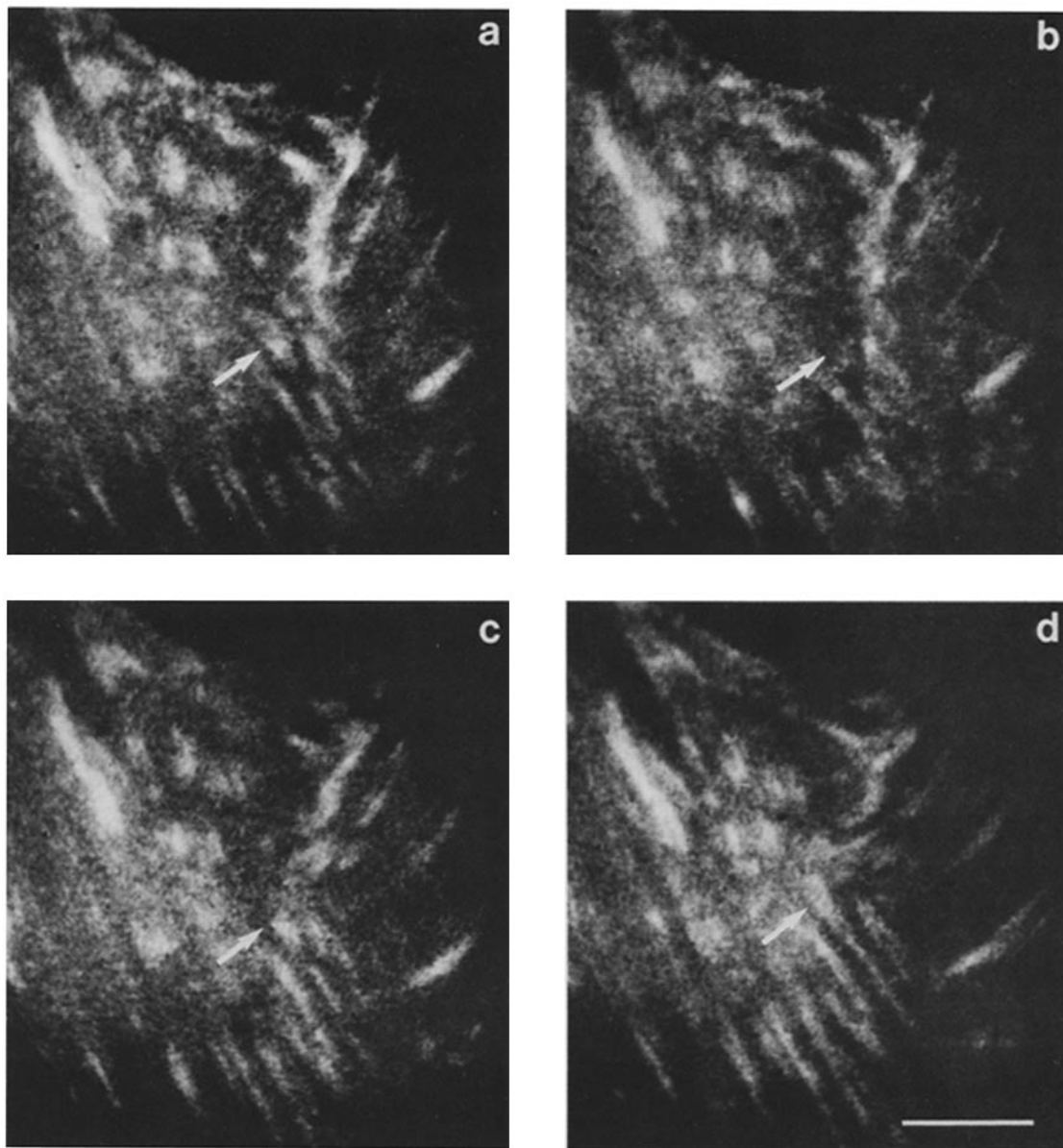
FIGURE 4 FRAP of an adhesion plaque in a fibroblast. Arrows indicate the location of the bleached spot. Recovery is complete within 20 min after bleaching (d). Fluorescence intensity before bleaching is designated 100% (a). Immediately after bleaching (b), fluorescence intensity equals 48%; 5 min after (c), 63%; 20 min (d), 97%. Bar, 10 μm.

Photobleaching of punctate structures yielded results similar to those for Z-lines. Initial recovery was detected soon after photobleaching, but complete recovery was not observed even after 6 to 7 h (Figs. 6 and 7).

Photobleaching of bundle-like structures revealed two classes of recovery. One had slow kinetics very similar to those of Z-lines and punctate structures (not shown). The other (hereafter referred to as stress fiber–like structures) had much faster kinetics (Figs. 6 and 8): complete recovery was detected within 60 min, a rate which is similar to that of stress fibers in fibroblasts. The $t_{1/2}$ for the stress fiber–like structures was ~9 min.

Except for the observation that stress fiber–like structures were generally shorter and thicker than slow-recovering bundles, the two classes of bundle-like structures were morphologically indistinguishable. Both were usually peripherally located and terminated near the edge of the cell. Their proximal ends were often continuous with lines of punctates or, less frequently, with myofibrils. When both a stress fiber–like bundle and an associated line of punctates were bleached, each structure recovered at its characteristic rate.

DISCUSSION

The recovery of alpha-actinin fluorescence in photobleached structures could reflect either direct exchange of photobleached alpha-actinin molecules with unbleached molecules present in the cytoplasm, or redistribution of alpha-actinin within partially bleached structures. However, in the latter case, recovery would be expected to propagate from the edge of the bleached spot towards the center, a pattern which was not observed. Therefore, direct exchange of incorporated bleached molecules with unincorporated unbleached molecules is probably responsible for the observed recovery. A similar conclusion was reached previously regarding the ex-
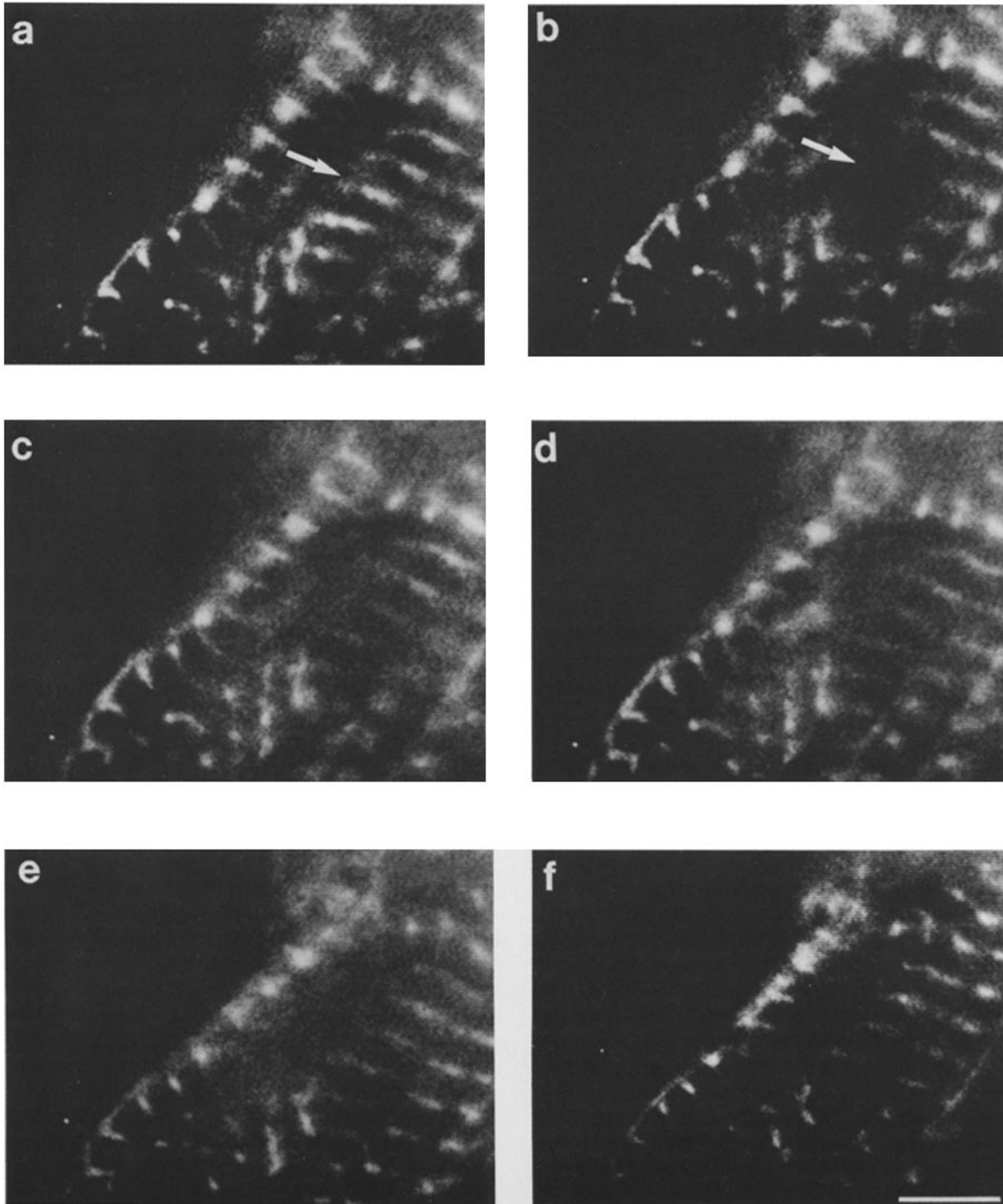
FIGURE 5 FRAP of Z-lines in a cardiac muscle cell. Arrows indicate the location of the bleached spot. Even after 6 ½ h, recovery is still incomplete (f). Fluorescence intensity before bleaching is designated 100% (a). Immediately after bleaching (b), fluorescence intensity equals 35%; 30 min after (c), 50%; 1 h (d), 61%; 4 h (e), 66%; 6 ½ h (f), 68%. Bar, 5 µm.
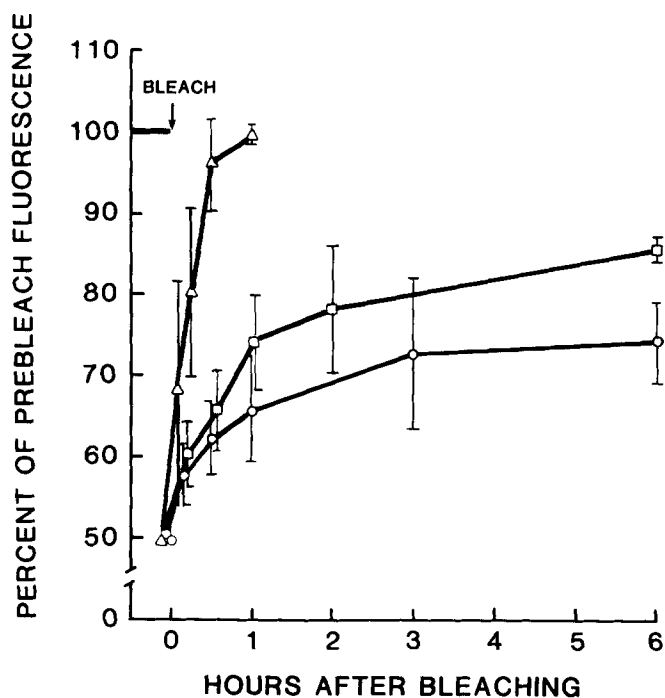
FIGURE 6 FRAP of structures in cardiac muscle cells as a function of time. Recovery of both Z-lines (O) and punctate structures (□) occurs very slowly and remains incomplete after 6 h, whereas recovery of stress fiber–like structures (△) is complete by ~1 h. Data have been normalized to an initial bleach level of 50%. Values are the means ± SDs of 5–15 experiments.

change of actin molecules along stress fibers (16). It is unlikely that the availability or diffusibility of alpha-actinin significantly affects the rate of recovery, since previous measurements have indicated a relatively high apparent diffusion coefficient for alpha-actinin in the ground cytoplasm (9), and since we have observed very different rates of recovery for structures in a single cell and even for structures which are continuous with each other. It is more likely that the rate of fluorescence recovery is determined by the rate at which alpha-actinin molecules associate with and dissociate from cellular structures.

While the initial incorporation of microinjected alpha-actinin took up to 3 h, FRAP required longer than 6–7 h for some structures in muscle cells. Presumably, microinjection of alpha-actinin upsets the equilibrium between the diffusible and incorporated pools of the protein, thus temporarily increasing the rate of association of diffusible alpha-actinin with cellular structures. However, once equilibrium is re-established, it seems to remain stable since similar rates of fluorescence recovery were obtained at various time points after microinjection.

It is not surprising that alpha-actinin can undergo relatively rapid exchange in fibroblasts. Motile fibroblasts are capable of considerable reorganization of stress fibers (28). A dynamic association of alpha-actinin and other proteins with stress fibers and adhesion plaques would facilitate these rearrangements. Kreis et al. (16) have examined the FRAP of actin associated with stress fibers and adhesion plaques. They similarly reported a "virtually complete" recovery of fluorescence in both domains by 30–35 min. We have, however, detected different mobilities of alpha-actinin associated with stress fibers and with adhesion plaques. The difference may be

related to the different protein composition found in adhesion plaques and along stress fibers. For example, tropomyosin, which presumably stabilizes actin-containing structures, is not detectable in adhesion plaques (8).

On the other hand, our data clearly indicate that the association of alpha-actinin with most structures in muscle cells is highly stable. Preliminary data with microinjected actin also indicated a high degree of stability of actin associated with myofibrils. These results are consistent with the observation that reorganization of myofibrils, comparable to the reorganization of stress fibers (28), is not detectable even with prolonged time-lapse recording (McKenna, N. M., unpublished observations). Moreover, myofibrils, unlike stress fibers, have been reported to persist through cell division (4). A more stable association of alpha-actinin and actin, and possibly of other proteins, could also be in part responsible for the achievement of a much higher spatial order of proteins in myofibrils, despite the general similarity in the arrangement of many proteins in myofibrils and in stress fibers.

Based on an analysis of the association of fluorescently labeled alpha-actinin with extracted stress fibers and myofibrils, Sanger et al. (22, 23) concluded that alpha-actinin molecules are probably self-associating in both structures. However, the dramatic difference between the exchangeabilities of microinjected alpha-actinin in muscle and fibroblast structures suggests that, in living cells, alpha-actinin association may be affected by the molecular environment of specific structures. Direct or indirect interactions of alpha-actinin with other molecules such as desmin, which is present in Z-lines but not in stress fibers (17), may have a significant effect on the exchangeability of alpha-actinin molecules. The differences in protein composition, spatial order, and stability suggest that stress fibers do not simply represent minimyofibrils.

One of the most interesting aspects of the present study is the identification of structures with highly different alpha-actinin exchangeabilities within the same muscle cell. Cultured cardiac muscle cells often contain clearly differentiated sarcomeres in one region, and less differentiated structures such as punctates and bundle-like structures in other regions. Frequently, these structures appear to be continuous with each other. Sanger et al. (24) recently reported the observation of linear arrays of punctate structures in permeabilized cardiac muscle cells stained with fluorescent alpha-actinin, and in living cardiac muscle cells microinjected with alpha-actinin. They suggested that these punctates may represent nascent Z-lines. However, the existence of bundle-like structures was not described in this report, but has been reported by other investigators using different types of muscle cells (6, 19). Our finding that some of these bundle-like structures resemble stress fibers in alpha-actinin mobility, whereas other muscle structures show much lower mobilities, suggests that cardiac muscle cells contain structures which may have existed before differentiation, and that the fast recovering bundles may be developmentally related to other structures in muscle cells. Some authors have postulated that stress fiber–like structures may perform an organizing function or act as templates for developing sarcomeres (6, 19). Current studies using time-lapse recording in combination with fluorescent analogue cytochemistry should yield a definitive picture of interrelationships among various structures detected in developing muscle cells.
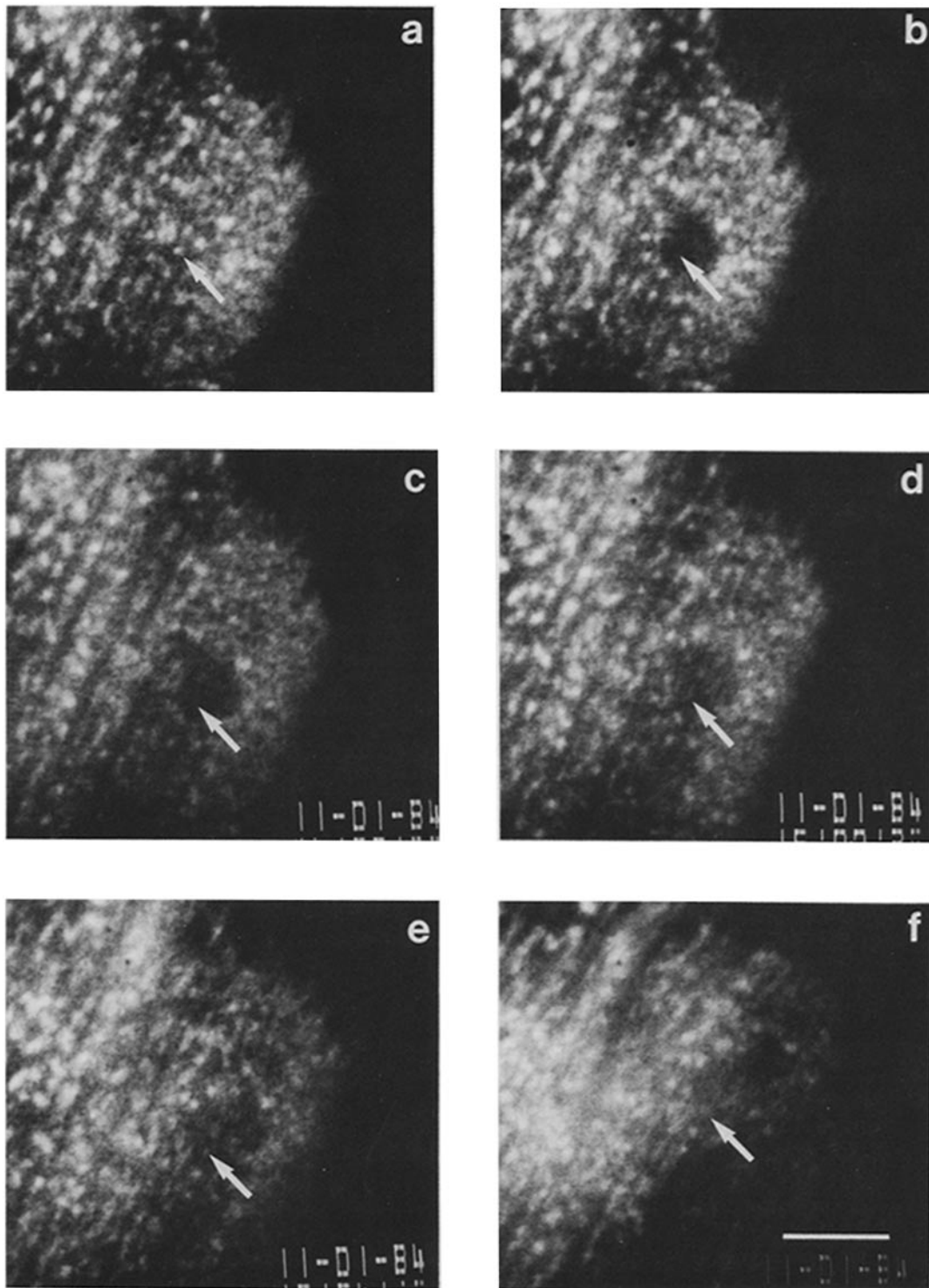
FIGURE 7   FRAP of punctate structures in a cardiac muscle cell. Arrows indicate a punctate structure bleached by the laser beam. Recovery is still incomplete 7 h after bleaching (f). Fluorescence intensity before bleaching is designated 100% (a). Immediately after bleaching (b), fluorescence intensity equals 28%; 30 min after (c), 51%; 2 h (d), 61%; 4 h (e), 69%; 7 h (f), 82%. Bar, 5 μm.
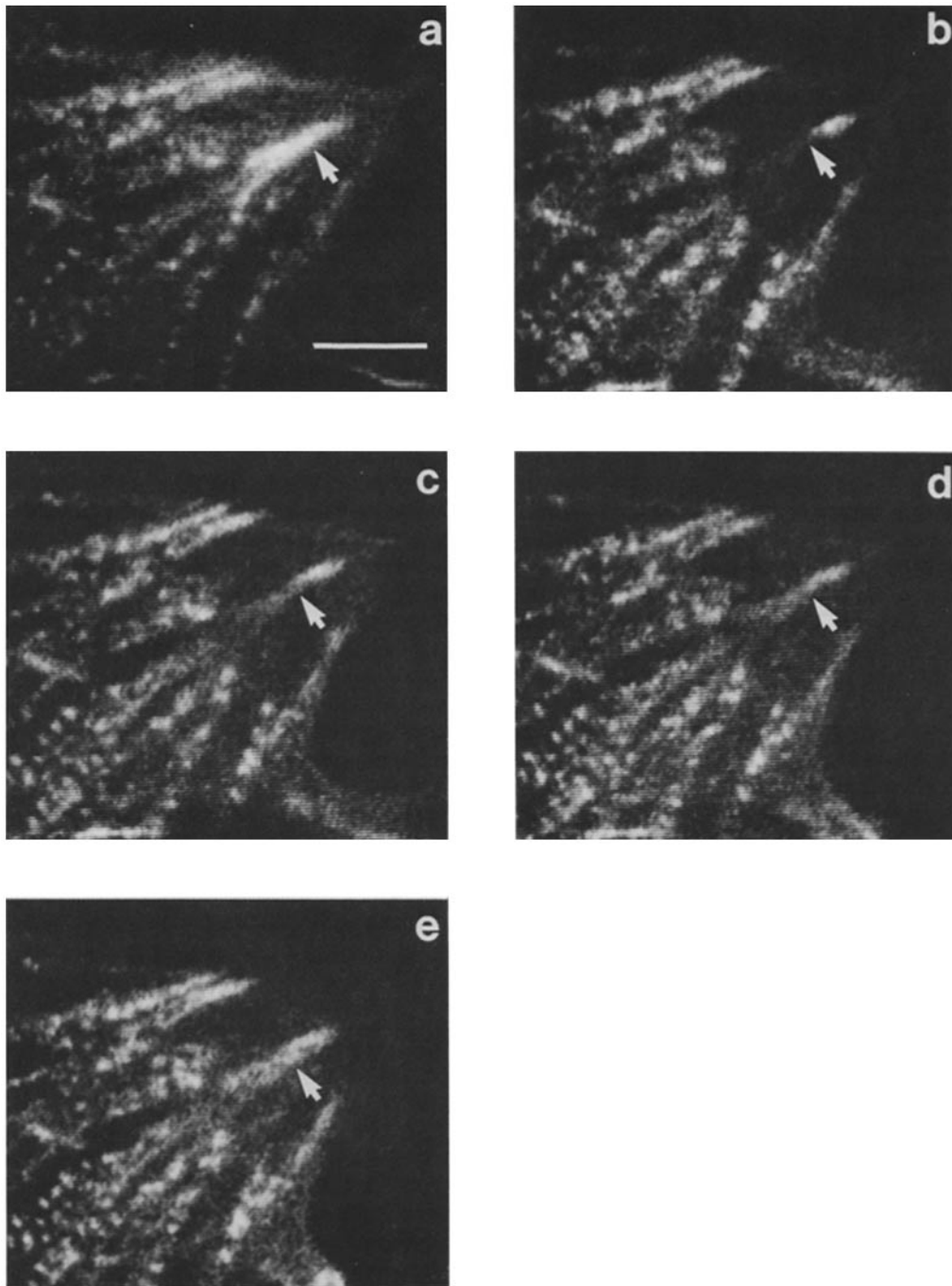
Figure 8 FRAP of a stress fiber–like structure in a cardiac muscle cell. Arrows indicate the location of the bleached spot. Essentially complete recovery is detected 60 min after bleaching (e). Fluorescence remains stable for several hours thereafter (not shown). Fluorescence intensity before bleaching is designated 100% (a). Immediately after bleaching, fluorescence intensity equals 37%; 15 min after (c), 64%; 30 min (d), 71%; 60 min (e), 95%. Bar, 5 μm.

REFERENCES

1. Amato, P. A., E. R. Unanue, and D. L. Taylor. 1983. Distribution of actin in spreading macrophages: a comparative study on living and fixed cells. *J. Cell Biol.* 96:750–761.
2. Begg, D. A., R. Rodewald, and L. I. Rebhun. 1978. The visualization of actin filament polarity in thin sections. *J. Cell Biol.* 79:846–852.
3. Burridge, K., and J. R. Feramisco. 1981. Alpha-actinin and vinculin from non-muscle cells: calcium-sensitive interactions with actin. *Cold Spring Harbor Symp. Quant. Biol.* 46:613–623.
4. Chacko, S. 1973. DNA synthesis, mitosis, and differentiation in cardiac myogenesis. *Dev. Biol.* 35:1–18.
5. Clark, W. A. 1976. Selective control of fibroblast proliferation and its effect on cardiac muscle differentiation in vitro. *Dev. Biol.* 52:263–282.
6. Dlugosz, A. A., P. B. Antin, V. T. Nachmias, and H. Holtzer. 1984. The relationship between stress fiber–like structures and nascent myofibrils in cultured cardiac myocytes. *J. Cell Biol.* 99:2268–2278.
7. Feramisco, J. R., and K. Burridge. 1980. A rapid purification of alpha-actinin, filamin, and a 130,000 dalton protein from smooth muscle. *J. Biol. Chem.* 255:1194–1199.
8. Geiger, B. 1979. A 130K protein from chicken gizzard: its localization at the termini of microfilament bundles in cultured chicken cells. *Cell.* 18:193–205.
9. Geiger, B., Z. Avnur, G. Rinnerthaler, H. Hinssen, and V. J. Small. 1984. Microfilament-organizing centers in areas of cell contact: cytoskeletal interactions during cell attachment and locomotion. *J. Cell Biol.* 99(1, Pt. 2): 83s–91s.
10. Goldman, R. D., B. Chojnacki, and M.-J. Yerna. 1979. Ultrastructure of microfilament bundles in baby hamster kidney (BHK-21) cells. *J. Cell Biol.* 80:759–766.
11. Gordon, W. E., III. 1978. Immunofluorescent and ultrastructural studies of "sarcomeric" units in stress fibers of cultured non-muscle cells. *Exp. Cell Res.* 117:253–260.
12. Jacobson, K., Z. Derzko, E.-S. Wu, Y. Hou, and G. Poste. 1977. Measurement of the lateral mobility of cell surface components in single living cells by fluorescence recovery after photobleaching. *J. Supramol. Struct.* 5:565–576.
13. Jacobson, K., E. Elson, D. Koppel, and W. Webb. 1983. International workshop on the application of fluorescence photobleaching techniques to problems in cell biology. *Fed. Proc.* 42:72–79.
14. Koonce, M. P., K. R. Strahs, and M. W. Berns. 1982. Repair of laser-severed stress fibers in myocardial non-muscle cells. *Exp. Cell Res.* 141:375–384.
15. Kreis, T. E., and W. Birchmeier. 1981. Stress fiber sarcomeres of fibroblasts are contractile. *Cell.* 22:555–561.
16. Kreis, T. E., B. Geiger, and J. Schlessinger. 1982. Mobility of microinjected rhodamine actin within living chicken gizzard cells determined by fluorescence photobleaching recovery. *Cell.* 29:835–845.
17. Lazarides, E., B. L. Granger, D. L. Gard, C. M. O'Connor, J. Breckler, M. Price, and S. I. Danto. 1981. Desmin-and vimentin-containing filaments and their role in the assembly of the Z disk in muscle cells. *Cold Spring Harbor Symp. Quant. Biol.* 46:351–378.
18. MacLean-Fletcher, S. D., and T. D. Pollard. 1980. Viscometric analysis of the gelation of Acanthamoeba extracts and purification of two gelation factors. *J. Cell Biol.* 85:414–428.
19. Peng, H. B., J. Wolosewick, and P.-C. Cheng. 1981. The development of myofibrils in cultured muscle cells: a whole mount and thin section electron microscope study. *Dev. Biol.* 88:121–136.
20. Salmon, E. D., R. J. Leslie, W. M. Saxton, M. L. Karow, and J. R. McIntosh. 1984. Spindle microtubule dynamics in sea urchin embryos: analysis using a fluorescein-labeled tubulin and measurements of fluorescence redistribution after laser photobleaching. *J. Cell Biol.* 99:2165–2174.
21. Sanger, J. W., J. M. Sanger, and B. M. Jockusch. 1983. Differences in the stress fibers between fibroblasts and epithelial cells. *J. Cell Biol.* 96:961–969.
22. Sanger, J. W., B. Mittal, and J. M. Sanger. 1984. Analysis of myofibrillar structure and assembly using fluorescently labeled contractile proteins. *J. Cell Biol.* 98:825–833.
23. Sanger, J. W., B. Mittal, and J. M. Sanger. 1984. Interaction of fluorescently labeled contractile proteins with the cytoskeleton in cell models. *J. Cell Biol.* 99:918–928.
24. Sanger, J. W., B. Mittal, and J. M. Sanger. 1984. Formation of myofibrils in spreading chick cardiac myocytes. *Cell Motility.* 4:405–416.
25. Saxton, W. M., D. L. Stemple, R. J. Leslie, E. D. Salmon, M. Zavortink, and J. R. McIntosh. 1984. Tubulin dynamics in cultured mammalian cells. *J. Cell Biol.* 99:2175–2186.
26. Taylor, D. L., P. A. Amato, K. Luby-Phelps, and P. McNeil. 1984. Fluorescent analog cytochemistry. *Trends Biochem. Sci.* 9:88–91.
27. Wang, K., J. R. Feramisco, and J. F. Ash. 1982. Fluorescent localization of contractile proteins in tissue culture cells. *Methods Enzymol.* 85:514–562.
28. Wang, Y.-L. 1984. Reorganization of actin filament bundles in living fibroblasts. *J. Cell Biol.* 99:1478–1485.
29. Wang, Y.-L., J. M. Heiple, and D. L. Taylor. 1981. Fluorescent analog cytochemistry of contractile proteins. *Methods Cell Biol.* 25(Pt. B):1–11.
30. Wang, Y.-L., F. Lanni, P. L. McNeil, B. R. Ware, and D. L. Taylor. 1982. Mobility of cytoplasmic and membrane associated actin in living cells. *Proc. Natl. Acad. Sci. USA.* 79:4660–4664.